NMR IN BIOMEDICINE, VOL. 7, 12–20 (1994)

Spin-Echo and Gradient-Echo EPI of Human Brain Activation using BOLD Contrast: a Comparative Study at 1.5 T

Peter A. Bandettini, Eric C. Wong, A. Jesmanowicz, R. Scott Hinks† and James S. Hyde*

Biophysics Research Institute, Medical College of Wisconsin, Milwaukee, WI 53226, USA and †Applied Science Laboratory, G.E. Medical Systems, Milwaukee, WI 53201, USA

In this study, Blood Oxygenation Level Dependent (BOLD) contrast in the detection of human brain activation was compared between spin-echo and gradient-echo echo-planar sequences at 1.5 T. Time course series of spin-echo and gradient-echo images containing the primary motor cortex were collected during rest (no finger movement) and activation (finger movement). Each time course series was collected using a different *TE*. Resting and active state signal intensities at each *TE* were measured in identical regions in the motor cortex. From these data, resting and active state R_2 ($1/T_2$) and R_2^* ($1/T_2^*$) values were obtained. Across four subjects, brain activation produced an average R_2 change of -0.16 ± 0.02/s (±SE), and an average R_2^* change of -0.55 ± 0.08/s. The average $\Delta R_2^*/\Delta R_2$ ratio was 3.52 ± 0.56. The average gradient-echo/spin-echo ratio of activation-induced signal changes at the *TE* for maximal BOLD contrast for each sequence ($TE\approx T_2^*$ and T_2) was calculated to be 1.87 ± 0.40.

INTRODUCTION

Oxygenated hemoglobin has essentially the same susceptibility as water, but deoxygenated hemoglobin is less diamagnetic than water.[1–3] Microscopic B_0 field gradients in the vicinity of red blood cells and vessels are modulated by deoxyhemoglobin concentration changes. Magnetic field perturbations within a voxel cause a loss of phase coherence and therefore signal attenuation in T_2- or T_2^*-weighted sequences. It has been demonstrated that blood oxygenation changes modulate T_2^* and T_2 of blood[2–13] and perfused brain tissue.[4–7,14–19] This type of contrast is called Blood Oxygenation Level Dependent (BOLD) contrast.[7]

Local cerebral blood oxygenation is increased in association with neuronal activity.[20–23] Mathematical simulations[24–27] based upon simplified models of physiological changes that accompany neuronal activation (increased flow, volume and oxygenation) show agreement with results from studies that have shown that the activation-induced signal changes are *TE*[28–32] and field strength[28,29,33,34] dependent. In addition, larger changes in R_2^* (or $1/T_2^*$) than in R_2 (or $1/T_2$) have been observed.[30,31,34–38] Simulations predict that if vessels, modeled as infinite cylinders, are generally larger than the water diffusion distance in a *TE*, activation-induced ΔR_2^* will be greater than ΔR_2.

Because of the greater BOLD contrast observed, gradient-echo sequences were the first used for non-invasive MRI mapping of human brain activation.[28,39–41] Nevertheless, spin-echo sequences, while producing less BOLD contrast than gradient-echo sequences, may have several advantages. The irreversible dephasing that occurs as a result of diffusion of spins through susceptibility induced gradients is maximized with compartments having similar dimension to the diffusion distance in a *TE* (i.e., 2–7 μm radius).[24–27] For this reason, it is hypothesized that BOLD contrast arising from spin-echo sequences reflects changes in oxygenation in micro vessels in close vicinity to the activated tissue, and not large draining veins which may be distant from the activated brain tissue. A higher *functional* spatial resolution may therefore be obtained with the use of susceptibility-weighted spin-echo sequences.

Spin-echo sequences also suffer considerably less susceptibility-related signal dropout from macroscopic field offsets occurring within a voxel, such as in the case of a poorly shimmed magnet or at interfaces of air, bone and/or tissue. The limitation of susceptibility-related signal dropout in gradient-echo sequences increases with field strength and is especially problematic in the study of deep brain structures, due to the air/tissue interfaces at the base of the brain.

It has been demonstrated that spin-echo and offset spin-echo[42] techniques suffer from less pulsatility artifacts in large vessels. The reason for this is most likely that the slice-selective 180° pulse 10–100 ms after the initial 90° does not refocus rapidly flowing spins, therefore creating a signal void where artifactual signal changes would occur with the use of gradient-echo sequences.

Changes in R_2 in voxels containing large vessels, and therefore greater blood volume, may be large due to diffusion of water through gradients induced around individual erythrocytes *within* the vessels, irrespective of the diffusion of spins through gradients *around* vessels. This implies that if draining veins are large enough to fill a voxel, the intrinsic R_2 changes in the blood with oxygenation changes may cause significant signal changes in addition to changes around micro vessels in parenchyma.

Other unknowns about the nature of BOLD contrast in general are that blood velocity changes may affect R_2 and R_2^* regardless of oxygenation changes. An alter-

* Author to whom correspondence should be addressed.

Abbreviations used: BOLD, Blood Oxygenation Level Dependent; EPI, echo planar imaging.

CCC 0952–3480/94/010012–09

Received 18 October 1993
Accepted (revised) 2 November 1993

ation of the velocity of the red blood cells can be considered as similar to an alteration of the diffusion coefficient. From models of the susceptibility-induced dephasing effect, it is understood that the extent of dephasing that occurs is closely linked to the extent of diffusion of spins through the susceptibility-induced field gradients. Any alteration of the extent of diffusion of spins through gradients around individual red blood cells, caused by blood velocity changes, may cause alterations in T_2 and T_2^*.

It is also understood that flow changes accompanying neuronal activation alter the apparent T_1 of perfused tissue.[39] The use of short *TR* values and large flip angles may introduce sensitization to apparent T_1 changes in addition to T_2^* signal changes.[43] This may make interpretation of signal enhancement magnitude and location additionally problematic.

The precise nature of BOLD contrast is not entirely understood primarily because a relatively small amount of information is known about the control of human cerebral blood flow, volume and oxygenation with neuronal activation.

In this study, we observe, at 1.5 T, activation-induced changes in spin-echo and gradient-echo signal from identical regions in the motor cortex as a function of *TE*. From these results, we compare relaxation rate changes and changes in functional contrast between the two sequences. Comparisons are made with the biophysical models of the BOLD contrast effect. In addition, practical comparisons are made.

EXPERIMENTAL

Four subjects (three males, one female: 20–27 years) were imaged using single-shot spin-echo and gradient-echo echo planar imaging (EPI) on a standard 1.5 T GE Signa scanner (GE Medical Systems, Milwaukee, WI) equipped with an inserted three-axis balanced torque head gradient coil designed for rapid gradient switching.[44] A shielded quadrature elliptical endcapped transmit/receive birdcage RF coil[45] was used for high sensitivity whole brain imaging.

For each subject, 11–19 time courses of 100 sequential spin-echo or gradient-echo images of a single axial slice containing the primary motor cortex were obtained. A different *TE* value was used for each time course series. For the spin-echo time course series, *TE* ($kx, ky = 0, 0$) was varied from 40 to 200 ms, and for the gradient-echo time course series, *TE* was varied from 20 to 120 ms. Each image was obtained with a readout window of 40 ms and a sampling rate of 8 μs per complex point. Slice thickness = 15 mm, FOV = 24 cm and matrix size = 64 × 64. The voxel dimensions were 3.75 × 3.75 × 15 mm.

During each time course, the subjects were instructed to perform a motor cortex activation task of tapping each finger to thumb, bilaterally, in a sequential and self-paced manner. Care was taken so that tapping frequency and pressure remained constant throughout each imaging session. The timing of the activation alternated 20 s rest (three episodes) with 20 s movement (two episodes).

All measurements from spin-echo and gradient-echo time course series were made in each subject from the identical regions of interest obtained in the following manner: (i) assuming that the optimum functional contrast is obtained at $TE = T_2^*$ or T_2,[31,32,46] a spin-echo and a gradient-echo time course series in which *TE* was closest to T_2 (ca 100 ms) and T_2^* (ca 40 ms) was chosen from each set of time courses; (ii) temporal cross-correlation was calculated on each of the two time course series[47] against the reference waveform illustrated in Fig. 1; (iii) for both time course series, all voxels which had a correlation coefficient <0.6 were removed. The cutoff value corresponded to a significance threshold of $p = 0.0001$, assuming Gaussian noise; (iv) voxels common to both the spin-echo and gradient-echo correlation coefficient images, after thresholding, were used as the region of interest for all of the spin-echo and gradient-echo time course series for each subject. Figure 2 illustrates the slice chosen for each subject and the region of interest used (superimposed in white) for all measurements. Note that the regions of interest corresponded closely to the primary motor cortices. Activated regions of interest from subjects 1–4, corresponding to Figs 2(a)–(d), contained 43, 38, 24 and 15 voxels, respectively.

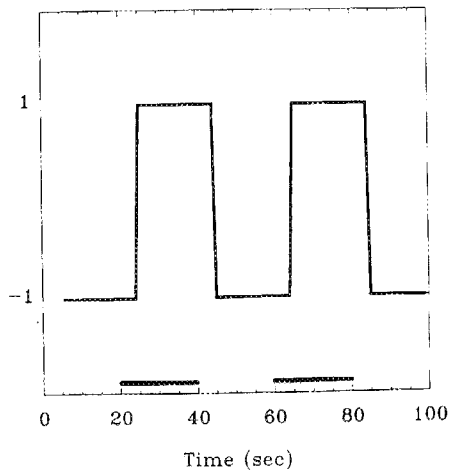

Figure 1. Illustration of the reference waveform that was used for all temporal cross-correlation calculations (images in Fig. 7) and temporal correlation coefficient calculations (activation masks in Fig. 2). The horizontal bars at the bottom indicate the periods during which subjects performed self-paced finger tapping. Because the activation-induced signal enhancement generally occurs ca 4–8 s after neuronal activation, a 5 s delay is introduced into the waveform analysis.

All measurements of resting and active state signal for spin-echo and gradient-echo sequences at each *TE* were made from the time course plots from the regions of interest. From these plots, points 10–20 were averaged to obtain the baseline signal and points 30–40 and 70–80 were averaged to obtain the activated state signal. A linear fit of the natural log of the signal intensities vs *TE* was used to obtain the respective relaxation rates during rest and activation.

RESULTS

Figure 3 illustrates three gradient-echo EPI time course plots from subject 4 at *TE* values ranging from 20 to 100 ms. Note that the per cent signal change shows an increase with increased *TE*. Figure 4 illustrates three spin-echo EPI time course plots from the same region

of interest at TE values ranging from 40 to 160 ms. The per cent signal changes also show an increase with increased TE, and, while easily observable, are significantly less than those observed in the gradient echo EPI time course series at corresponding TE values.

Figure 5 illustrates the T_2 and T_2^* decay curves for each subject. Error bars (±SE) are within the data points. As can be seen, a close correspondence to a single exponential decay was observed within the range of TE values used. The regions of interest used were likely to contain signal from cerebral spinal fluid, blood, gray matter and white matter. The T_2 rates are generally more consistent across the subjects than the T_2^* rates. This is most likely due to the sensitivity of T_2^* to variations in magnet shim and voxel size.

Table 1 summarizes the results shown in Fig. 5. Based upon differences in linear fits to the decay curves, significant ($p<0.05$) changes in R_2 were observed in two subjects and significant changes in R_2^* were observed in three subjects. The average value of ΔR_2 was -0.16 ± 0.02/s (±SE) and the average value of ΔR_2^* was -0.55 ± 0.08/s. The average ratio ($\Delta R_2^*/\Delta R_2$) of the relaxation rate changes was 3.52 ± 0.56. From this ratio, a comparison with a biophysical model was made to discern the vessel radius that predominantly contributed to the BOLD signal change. The model of Ogawa *et al.*[25] suggests that this relaxation rate ratio roughly corresponded to a vessel radius of ca 8 μm. Studies which have been performed to map, voxel for voxel, the relative changes in relaxation rates using a combined spin-echo and gradient-echo EPI sequence[36] have shown that the ratio of relaxation rates varies significantly across active voxels, suggesting that the predominant vascular scale contributing to BOLD contrast varies considerably in space. Relaxation rate mapping in a voxel by voxel manner may allow predominant vessel scale to be more accurately characterized.

It is potentially misleading to consider relative activation-induced relaxation rate changes between spin-echo and gradient-echo sequences as measures of the relative magnitudes of the BOLD contrast. If it is assumed that T_2 and T_2^* follow single exponentials, and that activation-induced ΔR_2 and ΔR_2^* are small compared to R_2 and R_2^*, the optimum TE for the detection of a maximal signal difference would occur at $TE\approx T_2^*$ for gradient-echo sequences and $TE\approx T_2$ for spin-echo sequences.[31,32,46] Table 1 shows R_2 and R_2^* related absolute signal changes calculated at optimum TE for every subject after normalizing the calculated signal to 1 at $TE=0$. The average signal difference ratio (gradient-echo/spin-echo) was calculated to be 1.87 ± 0.40 (±SE), which is considerably smaller than the relaxation rate change ratio.

Relative BOLD contrast changes with TE are illustrated in Figs 6 and 7. Figures 6(a) and (b) are the first images, from subject 4, at incremented TE values, in the gradient-echo and spin-echo time course series, respectively. Note that the signal decay in the gradient-echo images was not as spatially uniform as in the spin-echo images. The T_2^* decay rates differed not only

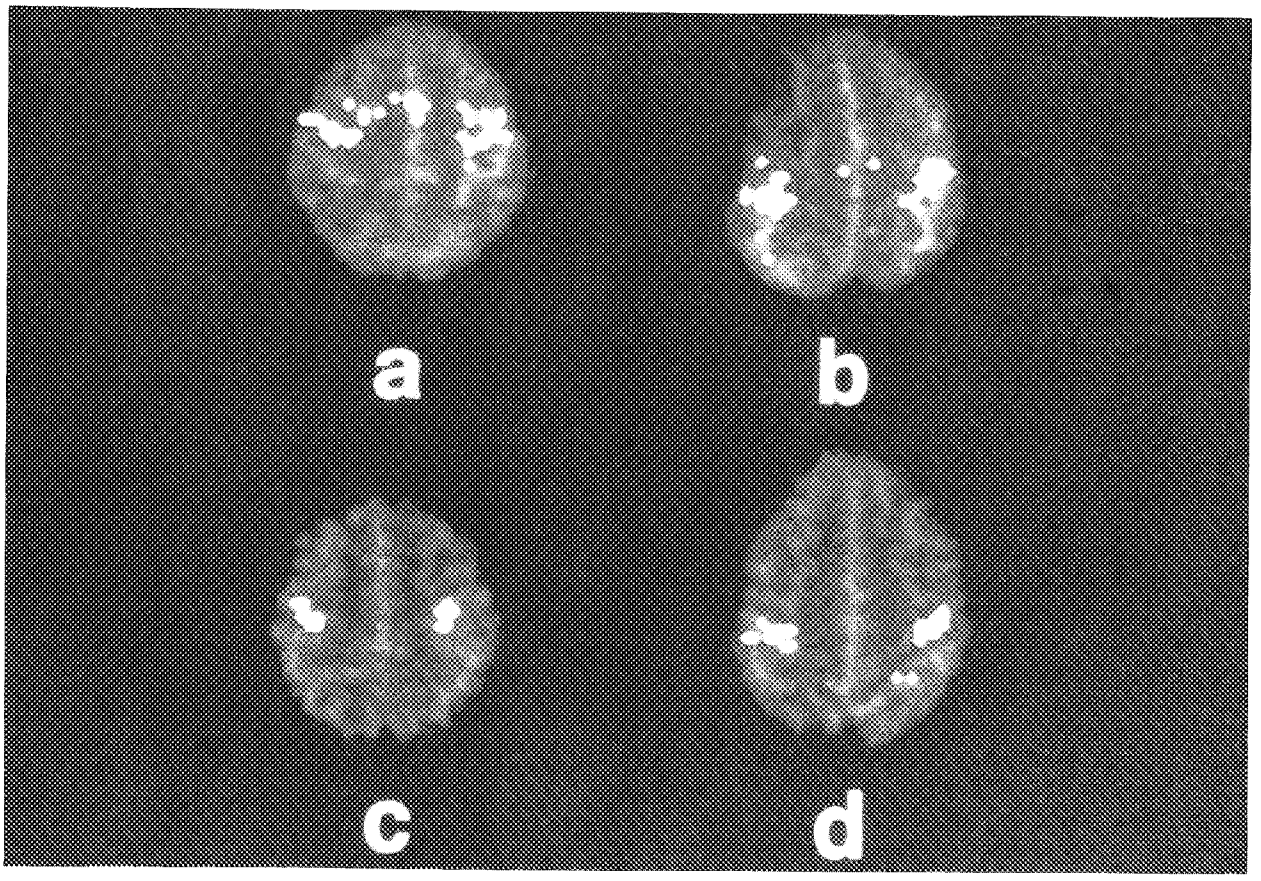

Figure 2. Spin-echo echo-planar images ($TE/TR=100/\infty$) of the axial slice chosen for each subject with the regions used for measurement superimposed in white. For selection of the regions of interest in each subject, two respective time course series were chosen from each set of time course series at TE values closest to the TE for maximal contrast ($TE\approx T_2^*$ and T_2). The regions are of the voxels that had a significant ($p<0.0001$) correlation with the reference waveform in Fig. 1 for a gradient-echo *and* a spin-echo activation time course series. Regions of interest in (a)–(d) corresponded to subjects 1–4, and contained 43, 38, 24 and 15 voxels, respectively.

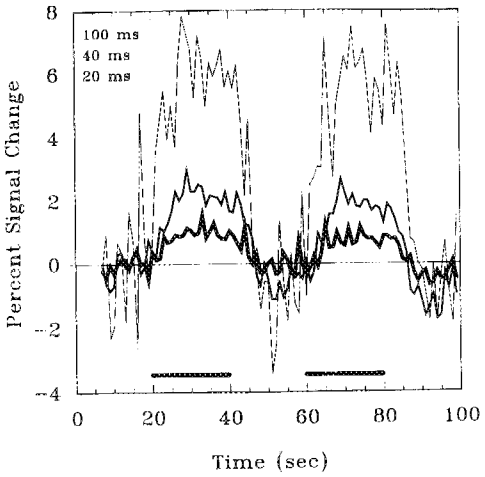

Figure 3. Three time course plots of the averaged signal from the region of interest in Fig. 2(d), obtained using gradient-echo EPI at *TE* values of 20 ms (most bold line) to 100 ms (lightest line). *TR* = 1000 ms. Horizontal bars at the bottom indicate when finger tapping was performed. The per cent signal change increases with *TE*.

between tissues but between areas having different B_0 field homogeneity. Figures 7(a) and (b) are correlation images from of gradient-echo and spin-echo sequences, respectively, corresponding to the anatomical images in Figs 6(a) and (b). They were obtained by scalar product

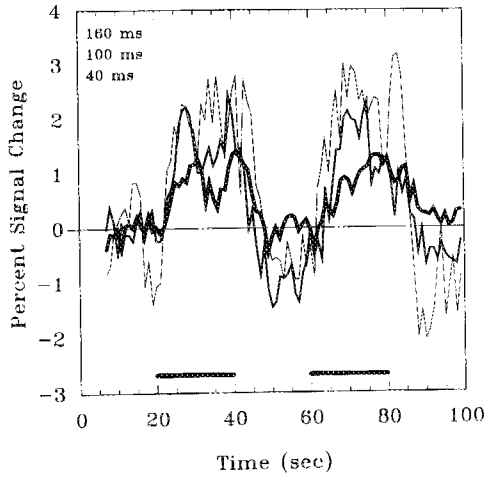

Figure 4. Three time course plots of the averaged signal from the region of interest in Fig. 2(d), obtained using gradient-echo EPI at *TE* values of 40 ms (most bold line) to 160 ms (lightest line). *TR* = 1000 ms. Horizontal bars at the bottom indicate when finger tapping was performed. The signal changes are easily seen and increase with *TE*, yet are much smaller than those observed at the corresponding *TE* values using gradient-echo EPI (Fig. 3).

calculation of the reference waveform, illustrated in Fig. 1, with every voxel in each time course series. No thresholding was applied. Figure 7(a) shows the gradient-echo correlation images. Signal enhancement is easily observed at short *TE* values, and the activation-induced signal changes with highest contrast to noise ratios are at *TE* values of 40–50 ms, which correspond to the T_2^* measurements from the region of interest [Fig. 5(d)]. At longer *TE* values, the signal decays into the noise, and activation-induced signal changes are therefore less readily apparent, even though the fractional signal change increases with *TE*. Figure 7(b) shows spin-echo correlation images. Overall, BOLD contrast was less than that produced by gradient-echo time course series, but was still high enough so that active regions were easily seen. Activation-induced BOLD contrast to noise appears to peak in the spin-echo sequences between 80 ms and 120 ms, which corresponds closely to the corresponding T_2 measurements from the region of interest [Fig. 5(d)].

DISCUSSION

MRI of human brain activation has been observed using spin-echo and gradient-echo EPI sequences. All active and resting state signals were obtained from the same region of interest in each subject. Identical brain activation timing and post processing methods were used to obtain resting and active state signals. From these signals, obtained using time course series with different *TE* values, relative R_2, R_2^*, ΔR_2 and ΔR_2^* rates were obtained. All calculations of relaxation rate change ratios and absolute signal difference ratios between gradient-echo and spin-echo sequences were based upon these measurements.

Because of the relatively large slice thickness and large regions of interest used, a substantial amount of partial voluming of active with inactive tissue probably occurred. The effect the slice thickness on the magnitude of activation-induced signal change has been studied.[48] Slice thicknesses on the order of the cortical thickness (3–4 mm) would prevent most partial voluming problems. The choice of slice thickness in this study was related, in part, to the uncertainty of the location and size of the activated motor cortex region in combination with the acquisition of only one slice. The large slice thickness most likely caused an underestimation of the absolute magnitudes of the relaxation rate changes

Table 1. Measured R_2 and R_2^* values from the resting and activated motor cortex (±SE) obtained from Fig. 5[a]

Subject	R_2 active (1/s)	R_2 resting (1/s)	R_2^* active (1/s)	R_2^* resting (1/s)	ΔR_2 (1/s)	ΔR_2^* (1/s)	$\Delta R_2^*/\Delta R_2$	at $TE = T_2$ calculated spin-echo ΔS	at $TE = T_2^*$ calculated gradient-echo ΔS	at $TE = T_2^*$ and T_2 calculated $\Delta S_{GE}/\Delta S_{SE}$
1	10.77±0.10	10.91±0.14	15.84±0.12	16.42±0.07	NS −0.13±0.07	** −0.58±0.08	4.35	0.0046	0.0133	2.89
2	10.86±0.13	11.01±0.17	26.83±0.25	27.26±0.13	** −0.14±0.04	NS −0.42±0.12	2.96	0.0048	0.0057	1.19
3	10.19±0.19	10.34±0.20	21.81±0.59	22.54±0.62	NS −0.16±0.12	** −0.75±0.04	4.56	0.0059	0.0124	2.10
4	11.31±0.19	11.51±0.20	19.29±0.20	19.72±0.22	** −0.20±0.03	** −0.44±0.04	2.21	0.0064	0.0082	1.28

[a] From these measurements, ΔR_2 and ΔR_2^* calculations are made. Significant differences in R_2 and R_2^* are indicated by **. Ratios of relaxation rate changes ($\Delta R_2^*/\Delta R_2$) are displayed. In addition normalized signal differences (at $TE = T_2$ or T_2^*), calculated from R_2 and ΔR_2 (spin-echo) and from R_2^* and ΔR_2^* (gradient-echo), are displayed. Gradient-echo/spin-echo signal difference ratios are displayed as a measure of relative BOLD contrast.

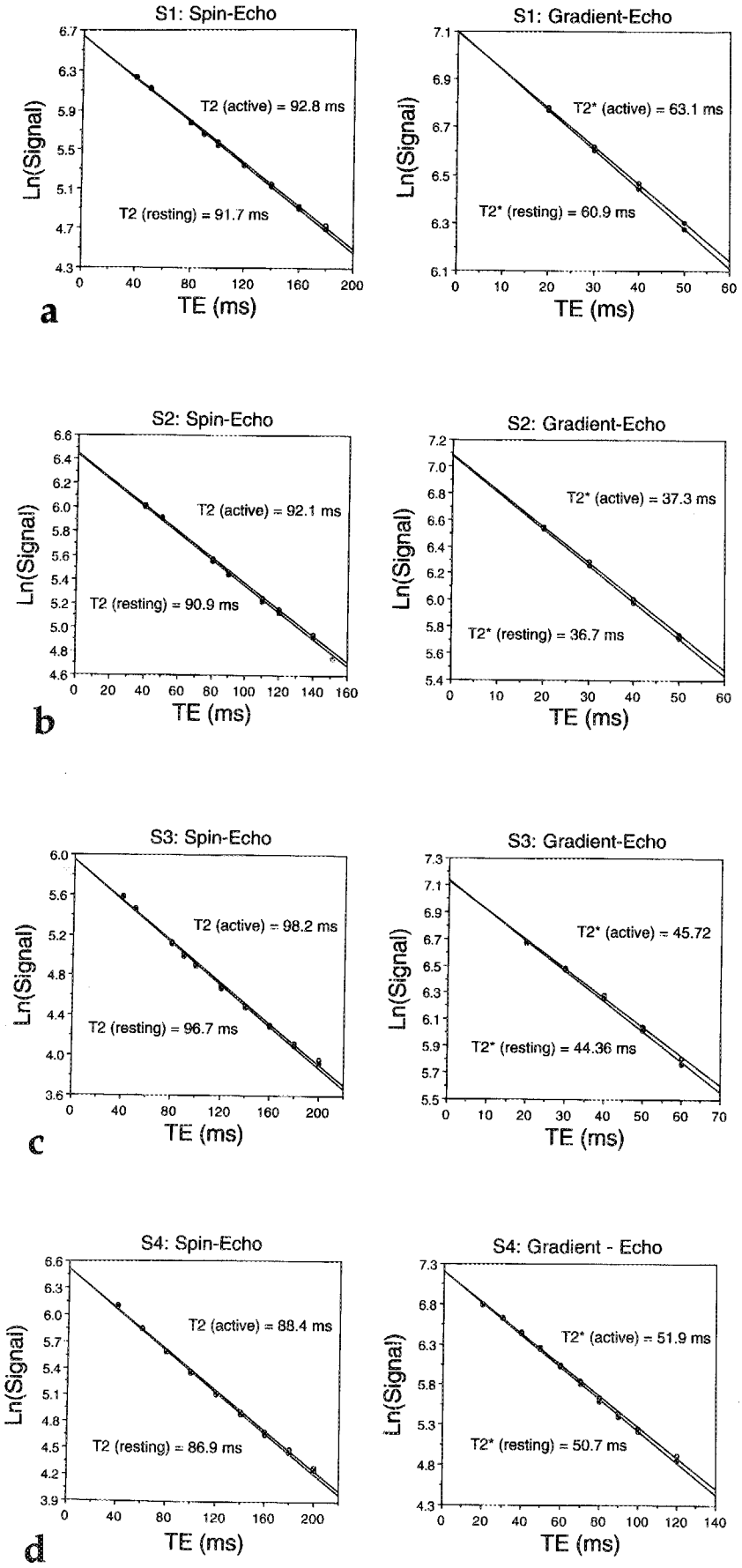

Figure 5. Resting and active state T_2 and T_2^* decay curves for subjects 1–4. (a)–(d) were created from time course plots of averaged signal from the regions of interest in Figs 2(a)–(d), respectively. From each time course plot, time points of 20–30 s were averaged for the resting state measurements. Time points of 30–40 and 70–80 were averaged for the active state measurements. Error bars are within most of the data points.

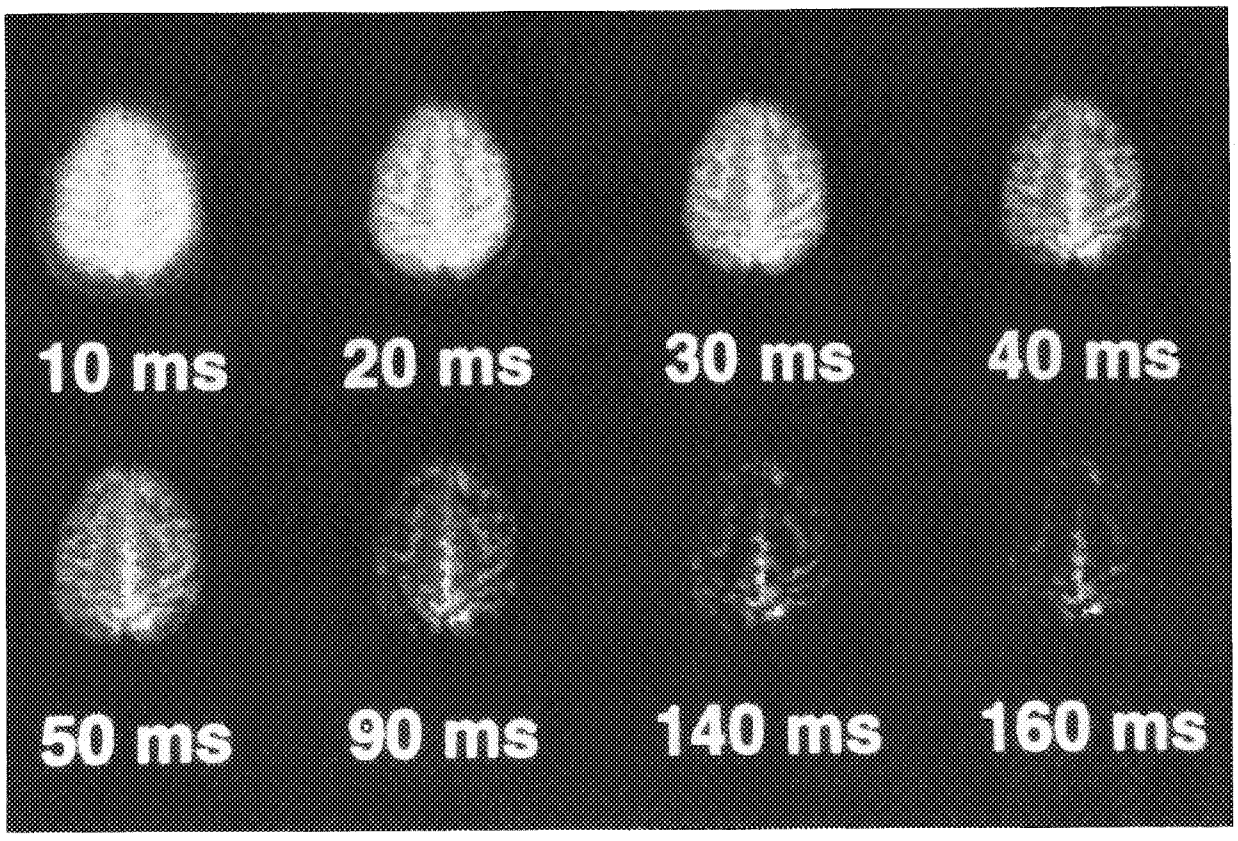

(a)

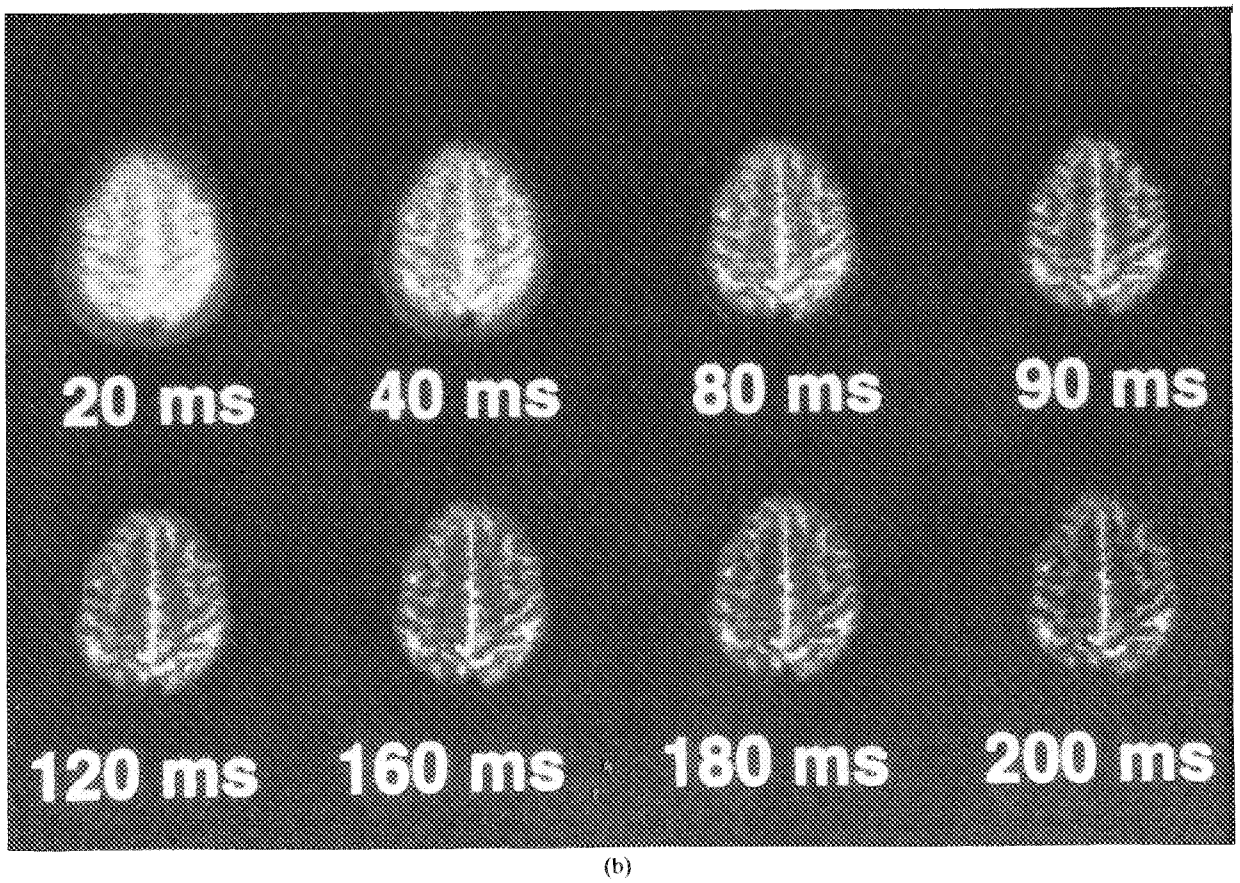

(b)

Figure 6. The first images ($TR = \infty$) in time course series from subject 4. (a) Gradient-echo images illustrate a rapid and spatially non-uniform decay of signal as TE is increased. (b) Spin-echo images illustrate a more uniform decay as TE is increased, demonstrating less signal dropout with variations in B_0 in the image.

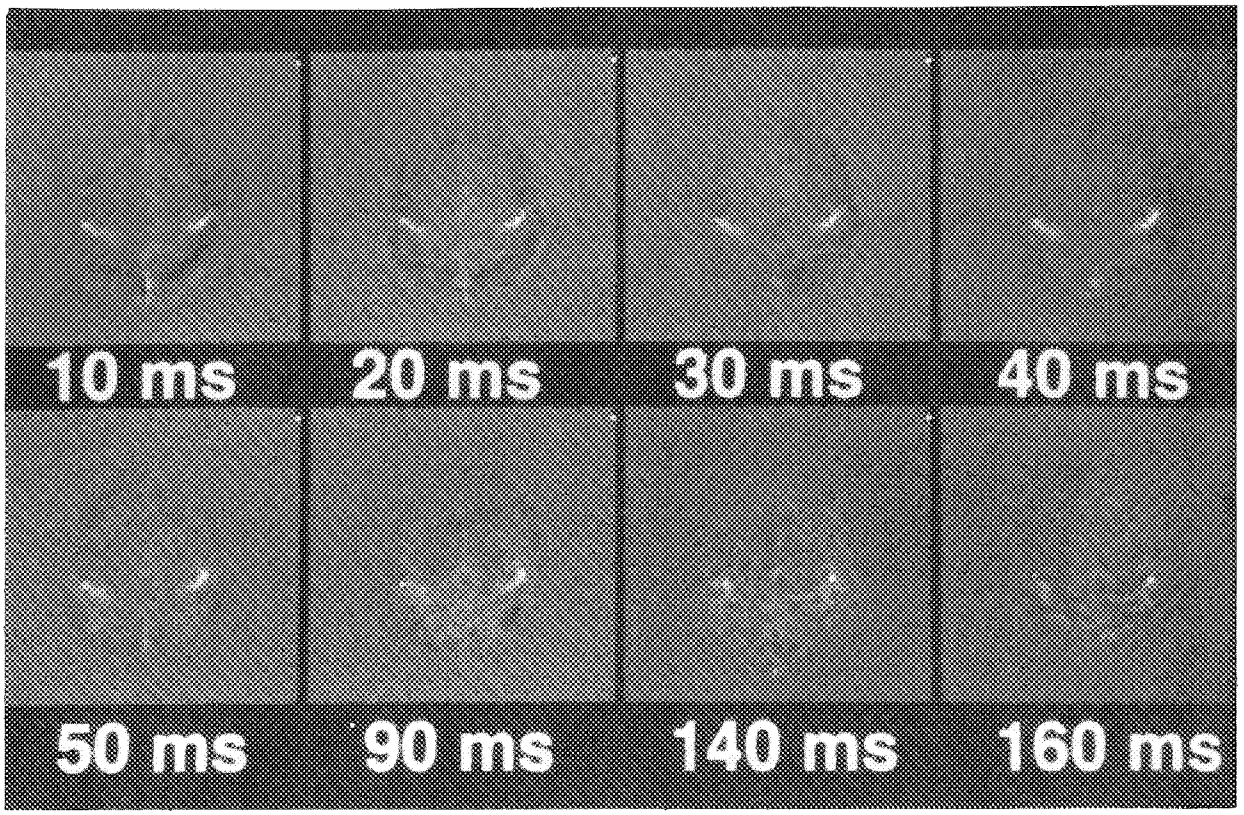

(a)

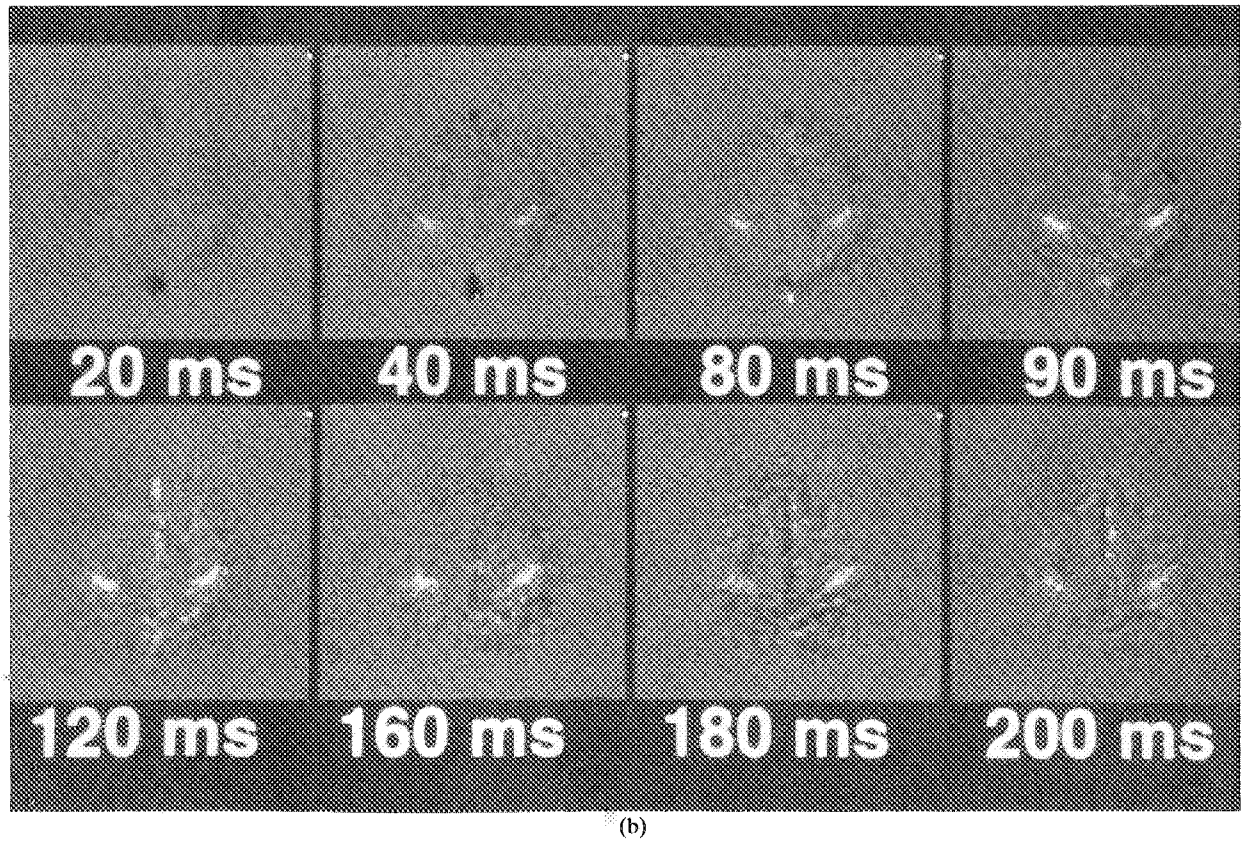

(b)

Figure 7. Brain activation images (bilateral motor cortex activation) obtained by temporal cross-correlation of the reference waveform in Fig. 1 with every voxel in the time course series. Images correspond to the anatomical images shown in Fig. 6. (a) Gradient-echo brain activation images demonstrate that the highest BOLD contrast to noise occurs at a *TE* in the range of the measured T_2^* values [Fig. 5(d)]. (b) Spin-echo brain activation images demonstrate that the highest BOLD contrast to noise occurs at a *TE* in the range of the measured T_2 values [Fig. 5(d)]. The spin-echo brain activation images have less BOLD contrast than the gradient-echo brain activation images. The active regions in the spin-echo images appear slightly more diffuse. Many areas showing signal enhancement are unique to either the spin-echo or gradient-echo brain activation images.

rather than the relative differences between spin-echo and gradient-echo sequences.

Potential errors involved with the comparison of spin-echo and gradient-echo activation-induced signal changes are many. Between time course series, activation timing and intensity may vary, and the subject may move or shift over the ca 2 h long scanning session. Artifactual signal changes in pulsatile vessels, which depend upon heartbeat timing relative to image acquisition timing, will vary from time course to time course. Analysis is underway in our laboratory with the use of a spatially and temporally registered gradient-echo and spin-echo EPI sequence to make more accurate comparisons, on a voxel by voxel basis, of relative relaxation rate changes and absolute signal changes with brain activation.[36]

One primary conclusion from this study is that the gradient-echo/spin-echo activation-induced BOLD contrast ratio is about 2 when considering the use of each pulse sequence at the optimal *TE* for detection of BOLD signal changes.

Spin-echo sequences are: (i) preferentially sensitized to smaller vessels; (ii) less sensitive to pulsatile flow artifacts; and (iii) less sensitive to macroscopic field gradients created by poor shim and tissue/brain/air interfaces. Although the intrinsic BOLD contrast is less in spin-echo sequences than in gradient-echo sequences, the advantages of less sensitivity to intravoxel dephasing in combination with sophisticated post processing techniques make spin-echo EPI a good alternative to gradient-echo EPI for functional activation studies. In addition, mathematical models predict that the ratio of BOLD contrast obtained using spin-echo and gradient-echo sequences may be closer to 1 at higher field strengths.[24–27]

From this comparative study, it is apparent that spin-echo techniques, sensitized to BOLD signal changes, show promise in the more extensive application of MRI to non-invasive assessment of human brain activation.

Acknowledgements

This work was supported, in part, by grants CA41464 and RR01008 from the National Institutes of Health. PAB thanks GE Medical Systems for financial support. Helpful discussions with Robert Cox and technical assistance from Lloyd Estkowski are greatly appreciated.

REFERENCES

1. Pauling, L. and Coryell, C. D. The magnetic properties and structure of hemoglobin, oxyhemoglobin, and carbonmonoxyhemoglobin. *Proc. Natl Acad. Sci. USA* **22**, 210–216 (1936).
2. Thulborn, K. R., Waterton, J. C., Matthews, P. M. and Radda, G. K. Oxygenation dependence of the transverse relaxation time of water protons in whole blood at high field. *Biochim. Biophys. Acta* **714**, 263–270 (1982).
3. Weisskoff, R. M. and Kiihne, S. MRI susceptometry: image-based measurement of absolute susceptibility of MR contrast agents and human blood. *Magn. Reson. Med.* **24**, 375–383 (1992).
4. Ogawa, S., Lee, T. M., Nayak, A. S. and Glynn, P. Oxygenation-sensitive contrast in magnetic resonance image of rodent brain at high magnetic fields. *Magn. Reson. Med.* **14**, 68–78 (1990).
5. Ogawa, S. and Lee, T. M. Magnetic resonance imaging of blood vessels at high-fields: *in vivo* and *in vitro* measurements and image simulation. *Magn. Reson. Med.* **16**, 9–18 (1990).
6. Ogawa, S., Lee, T. M. and Barrere, B. The sensitivity of magnetic resonance image signals of the rat brain to changes in the cerebral venous blood oxygenation. *Magn. Reson. Med.* **29**, 205–210 (1993).
7. Ogawa, S., Lee, T. M., Kay, A. R. and Tank, D. W. Brain magnetic resonance imaging with contrast dependent on blood oxygenation. *Proc. Natl Acad. Sci. USA* **87**, 9868–9872 (1990).
8. Brindle, K. M., Brown, F. F., Campbell, I. D., Grathwohl, C. and Kuchel, P. W. Application of spin-echo nuclear magnetic resonance to whole-cell systems. *Biochem. J.* **180**, 37–44 (1979).
9. Brooks, R. A. and Di Chiro, G. Magnetic resonance imaging of stationary blood: a review. *Med. Phys.* **14**, 903–913 (1987).
10. Gomori, J. M., Grossman, R. I., Yu-Ip, C. and Asakura, T. NMR relaxation times of blood: dependence on field strength, oxidation state, and cell integrity. *J. Comput. Assist. Tomogr.* **11**, 689–690 (1987).
11. Hayman, L. A., Ford, J. J., Taber, K. H., Saleem, A., Round, M. and Bryan, R. N. T_2 effect of hemoglobin concentration: assessment with *in vitro* MR spectroscopy. *Radiology* **168**, 489–491 (1988).
12. Weisskoff, R. M., Kiihne, S. R., Cohen, M. S. and Thulborn, K. R. Quantitative *in vivo* blood oxygenation measurements by echo planar imaging at 1.5 Tesla. *10th Annual Meeting of the Society of Magnetic Resonance in Medicine.* Abstr., p. 307 (1991).
13. Wright, G. A., Hu, B. S. and Macovski, A. Estimating oxygen saturation of blood *in vivo* with MR imaging at 1.5 T. *J. Magn. Reson. Imag.* **1**, 275–283 (1991).
14. Turner, R., LeBihan, D., Moonen, C. T., Despres, D. and Frank, J. Echo-planar time course MRI of cat brain oxygenation changes. *Magn. Reson. Med.* **22**, 159–166 (1991).
15. Hoppel, B. F., Weisskoff, R. M., Thulborn, K. R., Moore, J. and Rosen, B. R. Measurement of regional brain oxygenation state using echo planar linewidth mapping. *10th Annual Meeting of the Society of Magnetic Resonance in Medicine.* Abstr., p. 308 (1991).
16. Stehling, M. K., Schmitt, F. and Ladebeck, R. Echo-planar MR imaging of human brain oxygenation changes. *J. Magn. Reson. Imag.* **3**, 471–474 (1993).
17. de Crespigny, A. J., Tsuura, M. and Moseley, M. E. Real time detection of blood oxygenation changes during apnea in partially ischemic rat brain at 4.7 T. *11th Annual Meeting of the Society of Magnetic Resonance in Medicine.* Abstr., p. 914 (1992).
18. Jezzard, P., Heineman, F., Taylor, J., Despres, D., Wen, H. and Turner, R. Comparisons of EPI gradient-echo contrast changes in cat brain caused by respiratory challenges with direct spectrophotometric evaluation of cerebral oxygenation via a cranial window. *11th Annual Meeting of the Society of Magnetic Resonance in Medicine.* Abstr., p. 918 (1992).
19. Kwong, K., Hoppel, B., Weisskoff, R., Kiihne, S., Barrere, B., Moore, J., Poncelet, B., Rosen, B. and Thulborn, K. Regional cerebral tissue oxygenation studied with EPI at clinical field strengths. *J. Magn. Reson. Imag.* **2**, 44 (1992).
20. Cooper, R., Papakostopoulos, D. and Crow, H. J. Rapid changes of cortical oxygen associated with motor and cognitive function in man. In *Blood Flow and Metabolism in the Brain*, Vol. 1, pp. 14.8–14.9.
21. Fox, P. T. and Raichle, M. E. Focal physiological uncoupling of cerebral blood flow and oxidative metabolism during somatosensory stimulation in human subjects. *Proc. Natl Acad. Sci. USA* **83**, 1140–1144 (1986).
22. Frostig, R. D., Lieke, E. E., Ts'o, D. Y. and Grinvald, A. Cortical functional architecture and local coupling between neuronal activity and the microcirculation revealed by *in vivo* high-resolution optical imaging of intrinsic signals. *Proc. Natl Acad. Sci. USA* **87**, 6082–6086 (1990).
23. Villringer, A., Planck, J., Hock, C., Schleinkofer, L. and

Dirnagl, U. Near Infrared Spectroscopy (NIRS): a new tool to study hemodynamic changes during activation of brain function in human adults. *Neurosci. Lett.* **154**, 101–104 (1993).
24. Weisskoff, R. M., Hoppel, B. J. and Rosen, B. R. Signal changes in dynamic contrast studies: theory and experiment *in vivo*. *J. Magn. Reson. Imag.* **2**, 77 (1992).
25. Ogawa, S., Menon, R. S., Tank, D. W., Kim, S.-G., Merkle, H., Ellerman, J. M. and Ugurbil, K. Functional brain mapping by blood oxygenation level-dependent contrast magnetic resonance imaging. A comparison of signal characteristics with biophysical model. *Biophys. J.* **64**, 803–812 (1993).
26. Boxerman, J. L., Weisskoff, R. M., Hoppel, B. E. and Rosen, B. R. MR contrast due to microscopically heterogeneous magnetic susceptibility: cylindrical geometry. *12th Annual Meeting of the Society of Magnetic Resonance in Medicine.* Abstr., p. 389 (1993).
27. Wong, E. C. and Bandettini, P. A. A deterministic method for computer modelling of diffusion effects in MRI with application to BOLD contrast imaging. *12th Annual Meeting of the Society of Magnetic Resonance in Medicine.* Abstr., p. 10 (1993).
28. Ogawa, S., Tank, D. W., Menon, R., Ellermann, J. M., Kim, S.-G., Merkle, H. and Ugurbil, K. Intrinsic signal changes accompanying sensory stimulation: functional brain mapping with magnetic resonance imaging. *Proc. Natl Acad. Sci. USA* **89**, 5951–5955 (1992).
29. Frahm, J., Merboldt, K.-D. and Hänicke, W. Functional MRI of human brain activation at high spatial resolution. *Magn. Reson. Med.* **29**, 139–144 (1993).
30. Bandettini, P. A., Wong, E. C., Hinks, R. S., Estkowski, L. D. and Hyde, J. S. Quantification of changes in relaxation rates R_2* and R_2 in activated brain tissue. *11th Annual Meeting of the Society of Magnetic Resonance in Medicine.* Abstr., p. 719 (1992).
31. Bandettini, P. A., Wong, E. C., Estkowski, L., Hinks, R. S. and Hyde, J. S. Spin-echo echo-planar imaging of localized signal enhancement in the human brain during task activation. *J. Magn. Reson. Imag.* **3**, 63 (1993).
32. Menon, R., Ogawa, S., Tank, D. W. and Ugurbil, K. 4 Tesla gradient recalled echo characteristics of photic stimulation-induced signal changes in the human primary visual cortex. *Magn. Reson. Med.* **30**, 380–386 (1993).
33. Turner, R., Jezzard, P., Wen, H., Kwong, K. K., Le Bihan, D., Zeffiro, T. and Balaban, R. S. Functional mapping of the human visual cortex at 4 and 1.5 Tesla using deoxygenation contrast EPI. *Magn. Reson. Med.* **29**, 277–279 (1993).
34. Jesmanowicz, A., Bandettini, P. A., Wong, E. C., Tan, G. and Hyde, J. S. Spin-echo and gradient-echo EPI of human brain function at 3 Tesla. *12th Annual Meeting of the Society of Magnetic Resonance in Medicine.* Abstr., p. 390 (1993).
35. Hoppel, B. E., Baker, J. R., Weisskoff, R. M. and Rosen, B. R. The dynamic response of ΔR_2 and $\Delta R_2'$ during photic activation. *12th Annual Meeting of the Society of Magnetic Resonance in Medicine.* Abstr., p. 1384 (1993).
36. Bandettini, P. A., Wong, E. C., Jesmanowicz, A., Hinks, R. S. and Hyde, J. S. Simultaneous mapping of activation-induced ΔR_2* and ΔR_2 in the human brain using a combined gradient-echo and spin-echo EPI pulse sequence. *12th Annual Meeting of the Society of Magnetic Resonance in Medicine.* Abstr., p. 169 (1993).
37. Kwong, K. K., Chesler, D. A., Zuo, C. S., Boxerman, J. R., Baker, J. R., Chen, Y. C., Stern, C. E., Weisskoff, R. M. and Rosen, B. R. Spin-echo (T_2, T_1) studies for functional MRI. *12th Annual Meeting of the Society of Magnetic Resonance in Medicine.* Abstr., p. 172 (1993).
38. Turner, R., Jezzard, P., Le Bihan, D. and Prinster, A. Contrast mechanisms and vessel size effects in BOLD contrast functional neuroimaging. *12th Annual Meeting of the Society of Magnetic Resonance in Medicine.* Abstr., p. 173 (1993).
39. Kwong, K. K., Belliveau, J. W., Chesler, D. A., Goldberg, I. A., Weisskoff, R. M., Poncelet, B. P., Kennedy, D. N., Hoppel, B. E., Cohen, M. S., Turner, R., Cheng, H.-M., Brady, T. J. and Rosen, B. R. Dynamic magnetic resonance imaging of human brain activity during sensory stimulation. *Proc. Natl Acad. Sci. USA* **89**, 5675–5679 (1992).
40. Bandettini, P. A., Wong, E. C., Hinks, R. S., Tikofsky, R. S. and Hyde, J. S. Time course EPI of human brain function during task activation. *Magn. Reson. Med.* **25**, 390–397 (1992).
41. Frahm, J., Bruhn, H., Merboldt, K.-D. and Hänicke, W. Dynamic MR imaging of human brain oxygenation during rest and photic stimulation. *J. Magn. Reson. Imag.* **2**, 501–505 (1992).
42. Baker, J. R., Hoppel, B. E., Stern, C. E., Kwong, K. K., Weisskoff, R. M. and Rosen, B. R. Dynamic functional imaging of the complete human cortex using gradient-echo and asymmetric spin-echo echo-planar magnetic resonance imaging. *12th Annual Meeting of the Society of Magnetic Resonance in Medicine.* Abstr., p. 1400 (1993).
43. Frahm, J., Merboldt, K.-D. and Hanicke, W. Tissue vs vascular effects and changes of flow vs deoxyhemoglobin? Problems revealed by functional brain imaging at high spatial resolution. *12th Annual Meeting of the Society of Magnetic Resonance in Medicine.* Abstr., p. 1427 (1993).
44. Wong, E. C., Bandettini, P. A. and Hyde, J. S. Echo-planar imaging of the human brain using a three axis local gradient coil. *11th Annual Meeting of the Society of Magnetic Resonance in Medicine.* Abstr., p. 105 (1992).
45. Wong, E. C., Boskamp, E. and Hyde, J. S. A volume optimized quadrature elliptical endcap birdcage brain coil. *11th Annual Meeting of the Society of Magnetic Resonance in Medicine.* Abstr., p. 4015 (1992).
46. Blamire, A. M., Ogawa, S., Ugurbil, K., Rothman, D., McCarthy, G., Ellermann, J., Hyder, F., Rattner, Z. and Shulman, R. Dynamic mapping of the human visual cortex by high speed magnetic resonance imaging. *Proc. Natl Acad. Sci. USA* **89**, 11069–11073 (1992).
47. Bandettini, P. A., Jesmanowicz, A., Wong, E. C. and Hyde, J. S. Processing strategies for time-course data sets in functional MRI of the human brain. *Magn. Reson. Med.* **30**, 161–173 (1993).
48. Baker, J. R., Cohen, M. S., Stern, C. E., Kwong, K. K., Belliveau, J. W. and Rosen, B. R. The effect of slice thickness and echo time on the detection of signal changes during echo-planar functional neuroimaging. *11th Annual Meeting of the Society of Magnetic Resonance in Medicine.* Abstr., p. 1822 (1992).